Article

Modeling of a CO$_2$-Based Integrated Refrigeration System for Supermarkets

Ángel Á. Pardiñas [1],* , **Michael Jokiel [1]**, **Christian Schlemminger [1]**, **Håkon Selvnes [1]** and **Armin Hafner [2]**

[1] SINTEF Energy Research, Kolbjørn Hejes vei 1D, 7465 Trondheim, Norway; michael.jokiel@sintef.no (M.J.); christian.schlemminger@sintef.no (C.S.); hakon.selvnes@sintef.no (H.S.)

[2] Department of Energy and Process Engineering, Norwegian University of Science and Technology, Kolbjørn Hejes vei 1D, 7491 Trondheim, Norway; armin.hafner@ntnu.no

* Correspondence: angel.a.pardinas@sintef.no

Abstract: An integrated energy system that consists of a centralized refrigeration unit can deliver the entire HVAC&R (heating, ventilation, air conditioning, and refrigeration) demand for a supermarket. CO$_2$ (R744) is a natural refrigerant that is becoming increasingly popular for these centralized units due to significant energy and cost savings, while also being sustainable, safe, and non-toxic. This study focuses on the fully integrated CO$_2$ refrigeration system configuration for a supermarket in Porto de Mos, Portugal, which was equipped and fully monitored through the EU-funded project MultiPACK. A dynamic system model was developed in Modelica and validated against measurement data from the site recorded for one week. The model is used to provide additional ejector performance data supporting the obtained measurement data and to evaluate the system configuration at equivalent boundary conditions. The simulation results show that the installation of a vapor ejector (high-pressure lift) is sufficient to improve the efficiency of the unit compared to an ejector-less (high-pressure valve) system. However, more notable enhancements are achieved by including additional flooded evaporation with liquid ejectors and smart regulation of the receiver pressure, adding up to a global efficiency increase of 15% if compared to the high-pressure valve system during the validation week.

Keywords: Modelica; dynamic modeling; energy efficient; CO$_2$ commercial refrigeration; heat recovery; integrated refrigeration system; R744

1. Introduction

The global HVAC&R industry is facing an upcoming inevitable transition towards more energy-efficient solutions with minimal environmental impact, due to generally rising concerns for negative climate change impacts as well as due to new political legislations to lower global emissions in the near future. Following the F-gas Regulation and the Kigali amendment of the Montreal Protocol [1], commercial refrigeration has therefore been forced to rapidly increase efforts towards the application of alternative, eco-friendly solutions for replacing traditional systems. Using natural refrigerants such as CO$_2$, ammonia, and hydrocarbons represent the best long-term alternative for refrigeration systems due to their low environmental impact and no risk of being phased out in the future [2].

CO$_2$ has been proved [3,4] to be a reliable and sustainable alternative as a largely available solution for supermarkets after the F-gas phase-out in 2022. Nowadays, the preferred refrigerant choice for cooling and freezing equipment in European supermarkets is CO$_2$ systems. According to Shecco [5], the number of installed transcritical CO$_2$ units in May 2020 reached 29,000 installations in Europe and more than 35,000 worldwide. CO$_2$ technology is increasingly spreading beyond Europe to other regions as well, in particular to warm and hot countries where more conventional system layouts are not as efficient and where different technological advancements need to be implemented to enhance system efficiency.

In the EU-funded SuperSmart project, it was established that non-technological barriers such as general reluctance towards new technology can hinder further assimilation of energy-efficient CO_2 and ejector solutions in the HVAC&R and supermarket sector. Crucial non-technical barriers to overcome are the lack of knowledge of the technology among decision makers and the scarcity of properly trained service technicians and installers, highlighting the importance of training and knowledge exchange among technical and non-technical personnel in the refrigeration industry [6]. Knowledge transfer and training on CO_2 supermarket systems was one of the achievements of the SuperSmart project [7].

An example of technological advancement of CO_2 refrigeration systems is expansion work recovery with Multi-Ejector solutions, which make CO_2 systems further energy efficient compared to conventional synthetic refrigerant-based systems in common food retail applications [8,9]. The Multi-Ejector concept was extensively reviewed by [10], and it was concluded that the development and introduction of this technology have helped position all-in-one CO_2 supermarket refrigeration systems as a viable alternative to HFC-based systems in all climates. Several studies have shown that a single CO_2 (R744) refrigeration unit that combines HVAC and refrigeration systems is highly capable of replacing all the thermal energy services in food retail stores [11–14].

At the beginning of the CO_2 revival for use in the refrigeration sector in the 1990s, ref. [15] already introduced the idea of such integrated solutions that provide heating by heat recovery. As highlighted by the EU-funded H2020 MultiPACK project [16], units that are capable of providing refrigeration, air conditioning, and heating are nowadays available in the market. The general success of such integrated units is strictly related to their cost and performance competitiveness, as demonstrated in [8]. Ref. [17] documented field performances of CO_2 systems on a large scale and, based on these, developed suitable models to predict annual performances.

The project MultiPACK aims to demonstrate that integrated CO_2 refrigeration systems are an environmentally friendly alternative that can provide the best energy efficiency, reliability, and feasibility to boost a faster transition to low-environmental-impact solutions [18]. A thorough evaluation of the performance of all-in-one CO_2 supermarket systems using the multi-ejector configuration in warm climate conditions was identified as a key factor to support the proliferation of these systems across the world [19]. A confidence-raising campaign is therefore made in the course of the MultiPACK project [16], as confidence in the industry can mostly be raised by installing and monitoring fully integrated state-of-the-art systems in suitable climate regions such as South Europe. In the MultiPACK project, three state-of-the-art CO_2 systems for supermarkets in South Europe were installed, as described in [16]. These systems can supply all the required thermal energy needs of the site: Refrigeration, heating, cooling, and hot water production. The MultiPACK units include parallel compression, evaporator overfeeding, and ejectors for both expansion work recovery and liquid recirculation, together with AC and heat pump functionalities. MultiPACK units are scalable and adaptable to different requirements of the building's HVAC system.

The systems are furthermore equipped with a fully detailed monitoring infrastructure for both operation and performance evaluation to provide a wide range of measurement data. In close collaboration with a dynamic system model, the measurement data enable the possibility of evaluating the actual performance for each ejector group, i.e., high pressure (HP), low pressure (LP), and liquid ejector (LE), by running the system in different operating modes.

This study is based on an integrated CO_2 refrigeration unit that was installed in Porto de Mos (Portugal) within the context of the MultiPACK project. This unit aims to meet all the heating, cooling, and refrigeration demands of the supermarket with minimum energy consumption and is, for that purpose, equipped with different ejectors for expansion work recovery. The first main objective of this study is to validate a dynamic numerical model with experimental data from the location. The validated model is intended as a useful tool to analyze this ejector-supported integrated CO_2 refrigeration system in detail using a

dynamic numerical model validated with experimental data from the same location. With this strategy, it is possible to evaluate additional data, which cannot be determined with an experimental-only approach due to budget and space limitations. Another objective of this study is to use the numerical model to assess the efficiency improvement associated with the use of ejectors and different system layouts.

The energetic evaluation of the system performance of the different system layouts is therefore no longer restricted to the mere analysis of the available set of measurement data, which in addition, are dependent on external conditions at which these data were registered and cannot be controlled. Simulation results augment the knowledge gained from the system towards non-measured system components as well.

This article is structured as follows. Section 2 introduces the case study, illustrating the system layout, functionalities, measuring devices, and the general boundary conditions. Section 3 covers the modeling work that was conducted to assemble a Modelica model of the integrated CO_2 refrigeration system and the validation process with the measurement data from the field. Section 4 focuses on the results of the model validation process with measurement data from the field as well as on the dynamic simulation studies performed to evaluate the energy performance in the context of the expansion work recovery units. Conclusions and proposals for further work are indicated in Section 5.

2. Case-Study

2.1. System Layout

The integrated CO_2 refrigeration units installed in the frame of the MultiPACK project meet refrigeration (freezing and cooling), space heating, space cooling, and hot water production loads. The layout of the case study introduced in this paper is detailed in Figure 1. The system includes the main state-of-the-art technologies for CO_2 refrigeration units such as ejector-supported parallel compression, with ejectors for expansion work recovery and liquid ejectors for evaporator operation with minimized (or even zero) superheating, space heating, and air conditioning through CO_2-air rooftop units (RTUs), a heat pump mode evaporator, etc.

The compressor pack is an ejector-supported booster system with parallel compression. Three semi-hermetic compressors are installed at the medium temperature (MT) level, three compressors at the low temperature (LT) level, and there are four parallel compressors implemented mostly for air conditioning (AC), as detailed in Table 1. Smooth capacity modulation is achieved by inverter drives for one compressor per compressor level (30 to 60 Hz). The total installed electrical power for all compressors and auxiliary equipment (gas cooler/desuperheater fans, etc.) corresponds to 177 kW, excluding the fans for the RTUs.

Table 1. Bitzer compressors implemented in the system of the case study.

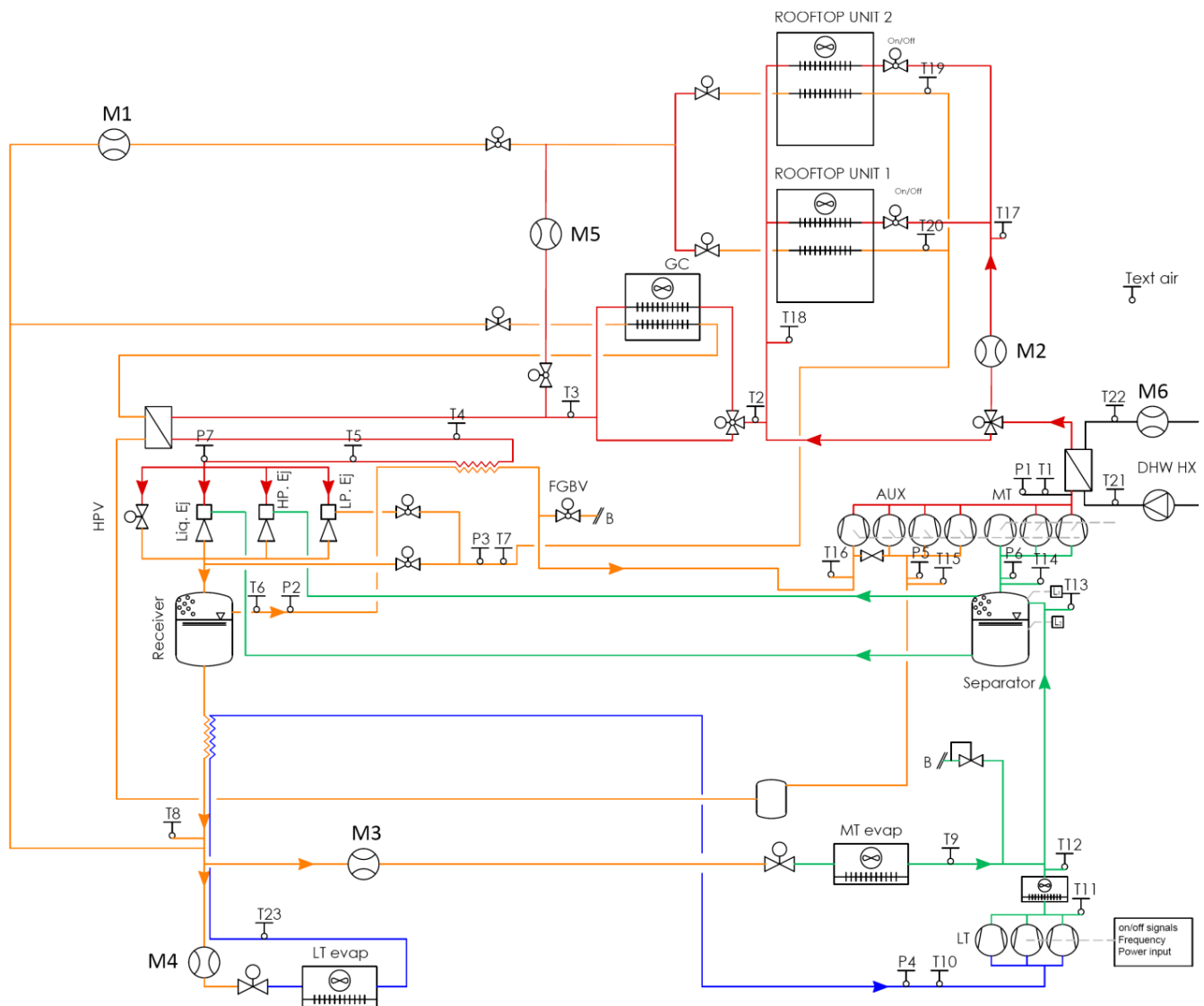| Compressor Group	Model	Displacement (m³/h) @50 Hz
MT	4HTC-20K 4FTC-30K (x2)	12.0 17.8
LT	2KSL-1K 2JSL-2K (x2)	2.71 3.48
AUX	4MTC-10K 4FTC-30K (x2) 6FTE-50K	6.5 17.8 26.1

Figure 1. System layout of the integrated CO_2 refrigeration system installed for the supermarket in Porto de Mos.

High-pressure CO_2 can be applied for heating domestic hot water (DHW) up to 60 °C before the remaining heat may be utilized in the RTUs. Excess heat of the CO_2 is then rejected to the ambient air by the gas cooler (GC), which can be partially or completely bypassed if needed.

The high-pressure stream is subcooled downstream of the gas cooler (and before the expansion devices) by the refrigerant sucked by the parallel compressors. Depending on the operation mode of the package, the expansion from a high-pressure level into the liquid receiver tank at an intermediate pressure level in the range of 35–45 bar is conducted by either the ejectors (high-pressure ejector or AC ejector) or by a high-pressure control valve (HPV). The ejectors implemented in the system are of fixed geometry and different sizes, arranged in blocks, and each ejector is enabled or disabled in a coordinated manner depending on the capacity requested (Multi Ejector concept by Danfoss [9]).

The liquid receiver separates flash gas and the liquid phase and accumulates the liquid to manage charge variations in the circuit and provide sufficient liquid head. The liquid CO_2 is subcooled and distributed to the LT, MT, and AC evaporators. The flash gas is either compressed by the AUX compressors or throttled by the flash gas bypass valve (FGBV) to the suction of the MT compressors, depending on the operating conditions.

The LT loads of the supermarket comprise cabinets, freezing rooms, and an ice machine. The liquid CO_2 mass flow supplied to the LT load is measured by a Coriolis mass flow meter, marked as M4 in Figure 1. The expansion to LT evaporation pressure is realized with electronic expansion valves separately controlled for each load. The low-pressure gas from the LT evaporators returns to the compressor pack with around 30 K superheat, and is heated further due to subcooling of the liquid CO_2, with this being the superheat at the suction of the LT compressors above 30 K. The refrigerant is then compressed from the LT pressure level to the MT separator pressure level.

The MT loads consist of open and closed cabinets and cold rooms, which are equipped with separate controlled electronic expansion valves. The supplied liquid CO_2 mass flow to the MT loads is measured by the Coriolis mass flow meter M3. A separator tank prevents liquid suction by the MT compressors. In case of excess liquid accumulation in the separator tank, a liquid ejector block is activated to return liquid to the receiver. The high-pressure ejector block recovers expansion work to suck part of the gaseous CO_2 from the separator tank back to the liquid receiver. This unloads the MT compressors in favor of the AUX (parallel) compressors, which operate with a lower pressure ratio.

The space heating and cooling demand of the supermarket is supplied by means of two rooftop units (RTUs). In the rooftop units, CO_2 directly flows into the heating and cooling coils. The arrangement of the rooftop units enables the usage of dehumidification. AC in the rooftop unit can be provided by either an ejector-supported AC operation or by utilizing direct expansion (DX) downstream from the GC:

- For the ejector-supported AC operation mode, an ejector block with low-pressure (LP) lift but a high entrainment ratio is utilized. In this case, the entire vapor of the AC evaporators is sucked by the LP ejector and lifted to the receiver pressure level. The Coriolis mass flow meter M1 measures the CO_2 mass flow rate for this AC operation mode.
- In the case of a DX AC mode, the Coriolis mass flow meter M5 is utilized to determine the CO_2 mass flow rate through the RTUs. The direct evaporation in the heat exchanger can be operated with ultra-low superheat. The increased flash gas amount during AC operation is handled by dedicated AC compressors.

The AC compressors can also be utilized for an additional heat rejection mode (i.e., heat pump mode). This mode can be activated when the heat that is available during the standard cooling mode is insufficient to completely cover the heating demand requested by the RTUs. The heat pump mode utilizes ambient air as a heat source for the separate set of coils in the gas cooler that operates as an evaporator with liquid CO_2 supplied by the liquid receiver. A solenoid valve is installed allowing independent heat pump functionality for some AC compressors, while others can still remove flash gas.

The MultiPACK demonstration site in Porto de Mos offers 2400 m^2 of air-conditioned area. The dimensioning refrigerant (evaporation temperature) and air (supply) temperatures and installed cooling capacities are listed in Table 2.

Table 2. Dimensioning temperatures and capacities for the integrated CO_2 refrigeration unit in Porto de Mos.

Service	Temperature	Capacity
LT	−30 °C	24 kW
MT	−4 °C	100 kW
AC (cooling)	10 °C	180 kW
AC (heating)	30 °C	160 kW

2.2. Measuring Devices

The system layout is fully instrumented to monitor operation modes and energetic performance in the field. The instrumentation comprises pressure transmitters, temperature sensors, refrigerant and water mass flow meters, the compressor input, and total power

meters. Figure 1 indicates the position of the sensors in the refrigeration system, while Table 3 indicates the types and accuracy of these devices. The status of every single compressor and the inverter frequency are also acquired. The liquid level in the liquid receiver is monitored to detect the status of the liquid ejectors since its activation depends on the liquid level in the receiver.

Table 3. Measurement devices implemented in the case study.

Device	Type	Precision
Temperature sensors (T)	NTC 10 kΩ	±0.5 K at 25 °C ($\pm$1.0 K from -40 °C to $+90$ °C)
Pressure transmitters (P)	Piezoresistive	±1% FS [a] = 60 bar ±4% FS = 150 bar
Power meters [b]	-	±0.5% FS
Refrigerant mass flow meters (M) [c]	Coriolis	±1% of reading
Water flow rate (M) [d]	Electromagnetic	±1% of reading

[a] FS = Full Scale, [b] Total of the pack (PTOT), LT compressors (PLT), MT compressors (PMT), AC compressors PAC), [c] M1 to M5. [d] M6.

The sampling rate corresponded to 60 s for most of the sensors, such as the pressure transmitters, temperature sensors, or compressor frequencies, and 120 s for the remaining sensors such as superheating, resulting in rather long time periods with unknown system performance that still need to be accurately calculated by the model. The data utilized in this study to validate the model described below were recorded during a summer week in 2019 (week 34). The integrated CO_2 refrigeration system was operated with a high-pressure (HP) ejector block and a disabled low-pressure lift (AC) ejector and liquid ejector, i.e., direct expansion RTU and dry expansion MT evaporators. This system configuration was selected to limit the variation in operational conditions of the system during the week and simplify the validation process. In a later stage, other operation modes will be considered.

3. Model Definition

3.1. Modeling the Integrated CO₂ Refrigeration System and Control Strategies

Figure 2 illustrates the Modelica model that was assembled to simulate the integrated CO_2 refrigeration system from Porto de Mos that is presented in Figure 1. The modeling work was carried out with the dynamic simulation software Dymola [20], using the object-oriented equation-based language Modelica [21] with model libraries called TIL and TIL Media [22]. TIL is a model library suitable for the stationary and transient simulation of thermodynamic systems while TIL Media contains a library including thermophysical properties for the utilized fluids [23]. Dynamic system modeling based on Modelica/Dymola can be used to quickly elaborate and test new system designs to prove their full potential for various applications. That way, the dimensioning of components and the control of system performance can be optimized, which enables more accurate assessments of operation modes for the integrated system.

A strong focus for the modeling job needs to be put on the controlling schemes. For highly dynamic system simulations such as this case study, the adjustment and tuning of the utilized controllers are of great importance for stable and reliable simulations. As an example, Figure 3 illustrates the existent highly dynamic boundary conditions for the system over a typical week in summer, with large fluctuations in the measured values for thermal demand loads or high pressure, which need to be covered by the implemented controllers.
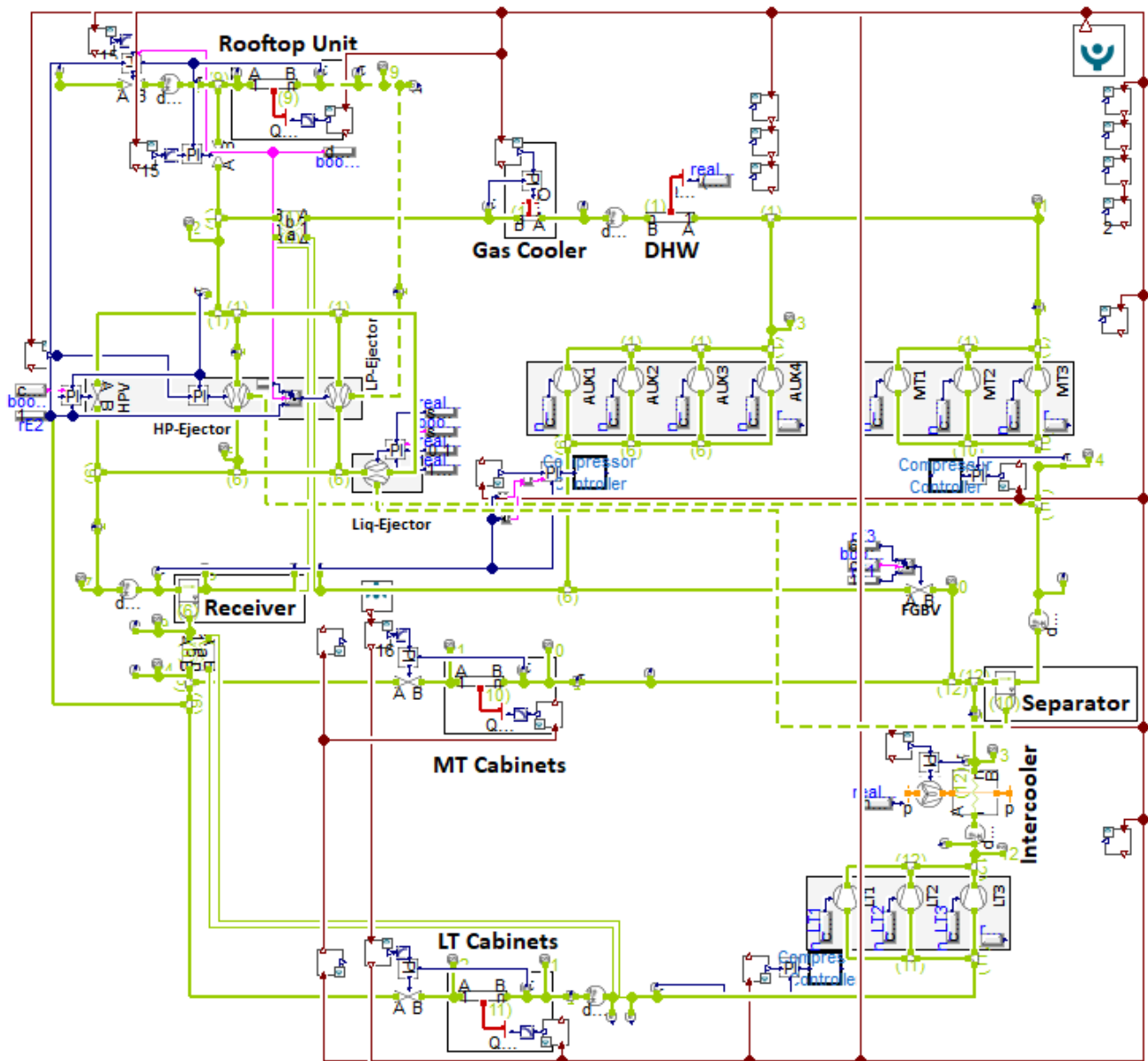
Figure 2. Layout of the Modelica model depicting the combined heating and cooling package of the Porto de Mos plant.

Regarding the control strategy for the integrated CO_2 refrigeration system in the model, a combination of measurement data and actual setpoints were used as setpoints for the PI controllers. The measurement data used as boundary conditions were the different thermal loads (DHW, AC, MT, and LT), as well as the gas cooler outlet temperature and high pressure. On the other hand, actual setpoints were implemented for each compressor suction pressure (or FGBV in the case of AUX compressors not in operation) and for the superheating degree of the different evaporators (15 K—MT, 15 K—AC, and 30 K—LT), controlled by the corresponding metering valves. This combined strategy was chosen over another based on setpoints only to better follow the real behavior of the supermarket and minimize the effect of the high sampling rate values on this validation.

The HP and LP ejectors both consist of two parallel ejector blocks, which in turn consist of six individual ejectors. The individual ejectors are thereby dimensioned with an increasing nozzle throat diameter, enabling an adjustment of the total ejector throttling area in discrete steps when single ejectors are constantly being switched on and off depending on the requested throttling capacity. However, the modeled ejectors are controlled with smooth adjustment of the total throttling area instead of discrete adjustment for numerical

stability reasons and to generally increase the simulation speed. More information is included in Section 3.3.
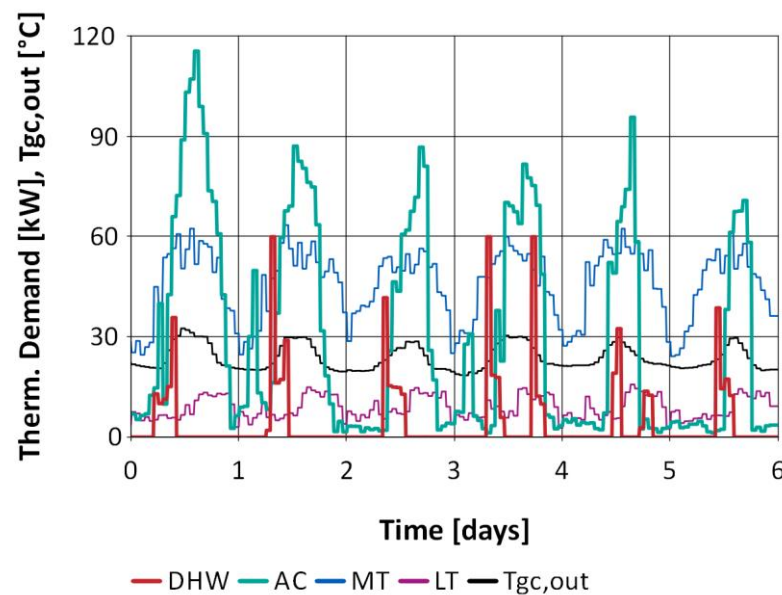

Figure 3. Measured values for thermal demands and system pressure for the integrated CO_2 refrigeration system in Porto de Mos during the evaluated week in summer 2019.

The set point for the HP and LP ejectors or the HPV, depending on the operation mode, was the measured pressure downstream of the gas cooler, i.e., the high-pressure side. For operation modes when the HP ejector is in use, the HPV is merely used as a safety device. For operation modes without HP ejector usage, the HPV is utilized to control the high pressure. The liquid ejector is only activated in case of a separator filling level of >90%, in order to return the liquid refrigerant in the separator to the receiver, being closed again at a separator filling level of <10%. During operation modes where the liquid ejector block is in principial in use, the superheating in the MT cabinet is greatly reduced, enabling the operation of flooded evaporation. This positively affects the MT evaporation temperature, which can be increased significantly. When applicable in the model, the setpoint was raised from $-9\,^\circ$C (27.2 bar) with the non-flooded operation, which was recorded during the test campaign, to $-4\,^\circ$C (31.3 bar) with the flooded operation, which was the setpoint considered in the design phase.

The calculated refrigeration and cooling loads were directly applied to the three evaporators (LT, MT, and AC) as fixed local boundary conditions. They could be evaluated based on the mass flow rate measurements available and the enthalpy differences in the evaporators, determined using the pressure transmitter and temperature sensors implemented. Values were recorded every minute and averaged over the time interval, i.e., 1 h.

All upstream valves leading to the three evaporators utilize the setpoints programmed in the real system controller. The AC load can be modelled either in the direct expansion mode or with the support of the LP ejector, as in the real case. Since the focus in this paper is on the HP ejector, only results with direct expansion are shown.

The following subsection describes the modelling strategy of compressors. Other aspects about the model are listed below:

- The receiver and separator were modelled as volumes of 600 L and 150 L, respectively.
- The amount of heat requested for domestic hot water (DHW) is calculated from the measured DHW values for water mass flow and inlet/outlet temperature for the DHX heat exchanger on the water side. In the model, the resulting DHW heat load is directly extracted from the CO_2, downstream of the MT and AUX compressors.
- The boundary conditions (thermal loads, temperatures, and pressures) used as inputs were retrieved by the model from csv files.

- The tubes between components are not modelled explicitly, even though there can be significantly different lengths in the real plant (liquid lines and suction lines to/from evaporators).
- The assumed loss-free refrigerant flow (no pressure drop in or between components).

3.2. Compressor Modeling

The Porto de Mos integrated CO_2 refrigeration system utilizes compressors from the manufacturer Bitzer. The performance of these compressors, i.e., compressor power consumption and mass flow rate, is available in the manufacturer's software [24] in the form of polynomial expressions according to the EN12900 standard [25]. The newly derived compressor models are based on such polynomials. The compressor packs are modeled in such a way that matches the real-world behavior as accurately as possible, with the compressors indicated in Table 1.

As for the compressor blocks, the compressors with the smallest capacity are always frequency-controlled in the range 30 to 60 Hz. The remaining compressors are on/off-controlled, which involves the control strategy following a sawtooth-shaped adjustment for the overall capacity, as shown in Figure 4. The controller of each compressor group uses the same value as the setpoint as that implemented in the real system. The MT compressor capacity is adjusted to match the MT evaporation temperature setpoint at −9 °C (or −4 °C with flooded evaporation). In the case of LT compressors, the LT evaporation setpoint is at −31 °C (the system was operated 1 K lower than the dimensioning value in Table 2). The AUX compressor capacity aims to control the receiver pressure according to the setpoint, which in the base case is 35 bar. However, the flash gas bypass valve (FGBV) is used when the amount of flash gas in the receiver is insufficient considering the compressors implemented.
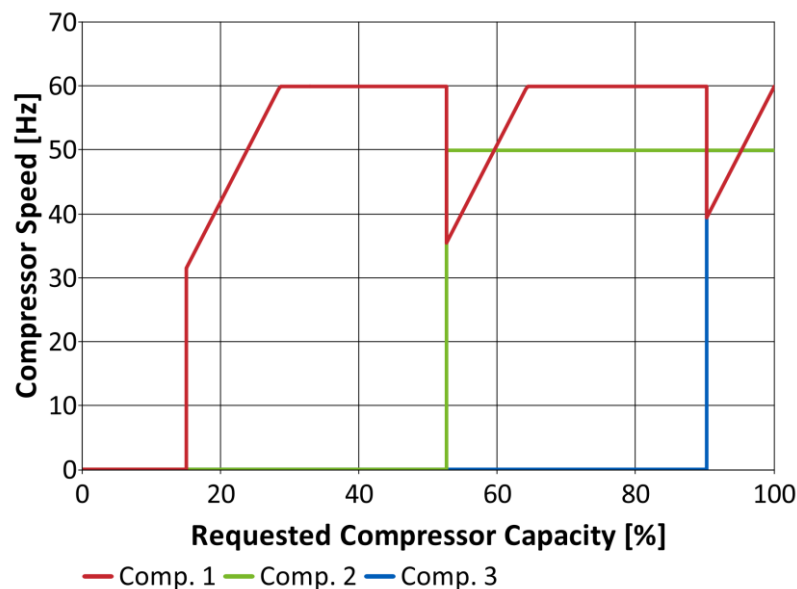

Figure 4. Course of the total compressor capacity resulting from both frequency- and on/off-controlled compressors (MT compressor group).

3.3. Ejector Model

Ejector modelling can be approached with different levels of complexity. The TIL libraries utilized in the Modelica models contain ejector models of relative simplicity. Among these options is the constant-efficiency-based model, where a nozzle model and constant ejector efficiency value need to be defined. The nozzle model relates the mass flow rate of primary flow with the cross-section area of the flow-restricting channel (opening degree). The ejector efficiency determines the pressure lift/entrainment ratio of the ejector and has been defined in works in the literature such as [26,27]. More complex and detailed

ejector models can be implemented, and an example was a result of the project SuperSmart-Rack [28], funded by the Research Council of Norway. This model is based on extensive sets of measurements including various ejector operation points [29–32]. The model implemented ".bin" files that contain the sets of measurement data. The model can be used as an ejector block with numerous parallel ejector cartridges operating in an on/off mode to adjust the total ejector nozzle area in a discrete way. In addition to the mere ejector model, sophisticated control blocks are implemented for switching the particular cartridges on and off, dependent on a given optimal high-pressure function. Figure 5 depicts the ejector efficiency map of the utilized ejector model in this study.
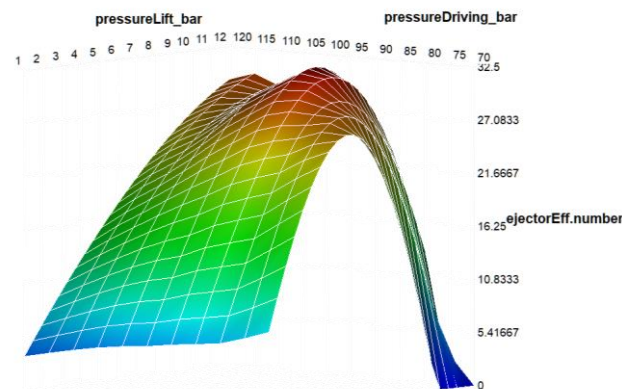

Figure 5. Ejector performance map for the utilized high-pressure lift ejector model in this study, illustrating the impact of pressure lift (from 1 to 12 bar) and driving pressure (from 70 to 120 bar) on the resulting ejector efficiency (from 0 to 32.5%).

The initial approximation in the present study was to conduct an ejector performance assessment in two steps. The first step was to conduct the dynamic simulations with the constant ejector efficiency models, using the well-validated Brennen correlation for the nozzle model [33] and two values of constant ejector efficiency equal to 15% and 30%. The second step was to evaluate the accuracy of the constant ejector efficiency approach. For this, the more detailed ejector model described in the previous paragraph was utilized in a tester with open boundaries for each ejector port (motive, suction, and discharge). The boundaries are supplied with recorded boundary conditions (pressures, enthalpies, and mass flow rates) from the system model with constant ejector efficiency. Implementing the detailed ejector model in the general system model was considered, but it resulted in highly increased computational time and effort, unacceptable for longer simulation runs.

The result of the two-step process can be summarized by Figure 6 (left-hand side) for a 24-h period. It shall be noted that the consideration of original values for the constant ejector efficiency (i.e., 30% and 15%) on the system level finally resulted in rather minor deviations for the actual ejector efficiency in the tester environment. Averaged efficiency values of 22.7% and 21.2% for the HP ejector block were obtained with the boundary conditions from the system simulation with constant ejector efficiencies of 30% and 15%, respectively. However, it is rather clear that with dynamic simulations, where mainly the motive nozzle conditions vary significantly, even if pressure lift is rather constant, this approach could be improved.

An intermediate solution between the simplified ejector model from the library and the detailed ejector model was adopted. On the one hand, a continuous adjustment of the motive nozzle cross-section area was allowed in order to avoid the numerical challenge caused by simulating the frequent switching of the parallel ejector cartridges. On the other hand, the ejector efficiency obtained from the detailed ejector model was approximated with a polynomial function of pressure lift and motive (driving) pressure of a structure similar to the compressor polynomials. The HP ejector efficiency could be correlated with $R^2 = 0.924$ in the range of pressure lifts from 1 to 12 bar and motive pressure from 70 to

120 bar. As shown in Figure 6 (right-hand side), there is good agreement between the results from the detailed model and the ejector efficiency with this polynomial approach.
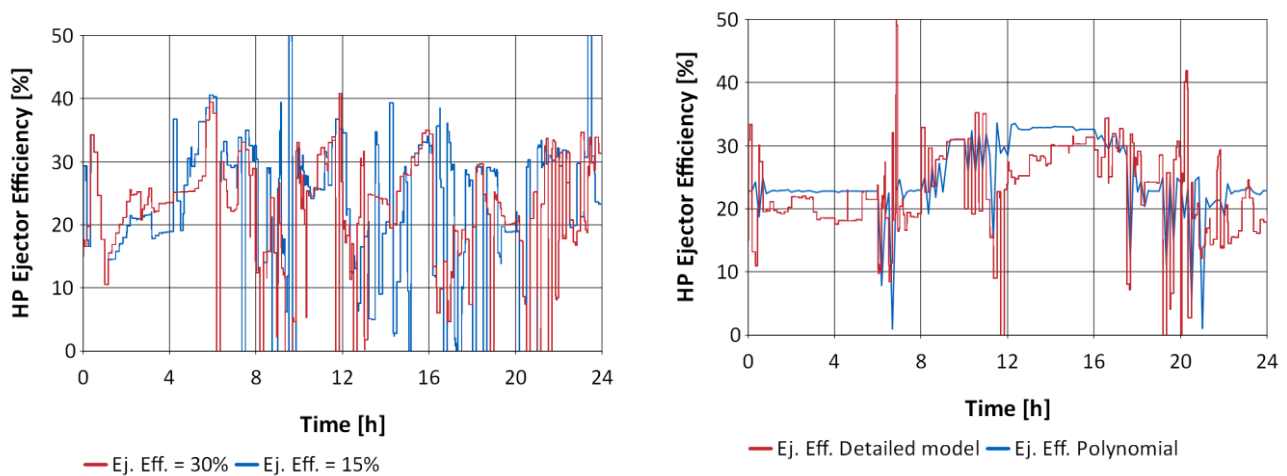

Figure 6. Calculated ejector efficiency for a standard operation period for the high-pressure ejectors with the detailed model, using boundary conditions from system simulations with constant ejector efficiency of originally 30% and 15% (**left**), and ejector efficiency based on polynomials after mapping the detailed model (**right**).

A special case is the liquid ejector, which is used occasionally to empty the separator when the MT evaporators are flooded when operated. Based on reference [9], it was decided to model the liquid ejector with a constant efficiency of 10%. The motive cross-section area was set as either fully closed or fully open, with no regulation in between.

4. Results and Discussion

4.1. Compressor Validation

The validation of the compressor models has been conducted in a tester environment where the compressor packs are embedded into boundary conditions that were directly taken from measurements. The inlet conditions of the compressors are provided by measured values for compressor inlet pressure and inlet enthalpy. The measured outlet pressure is provided for the outlet boundary. For this test case, the individual compressors are controlled by the measured values for compressor speed to be able to make assumptions on the quality of the implemented Bitzer polynomials. Figures 7 and 8 show the total compressor power consumption and compressor discharge temperatures that have been calculated by the model in comparison to the actual measurement values. It should be noted that the simulation results for the calculated compressor discharge temperature for MT and AUX compressors needed to be merged in Figure 8 (right), as the relevant temperature sensor (marked as "T1" in Figure 1) that is used for validation is located after the junction from both MT and AUX compressor outlets. A separate validation of MT and AUX compressors was therefore not possible with the existing measurement data.

It is concluded from this validation that the measured compressor power consumptions are well reproduced by the models. If anything, there is a slight, but acceptable, underestimation by the models, which could be explained by (i) the power consumption of the inverters driving the frequency-controlled compressors, which is not accounted for by the models, and (ii) the margin of accuracy inherent to the compressor polynomials according to the EN 12900 standard [25]. The discharge temperatures are overestimated by the model if compared to the measurements, by 4.5 K on average in the case of the LT compressors and approximately 6 K for the MT + AUX compressors. The reason for this mismatch is the fact that the temperature sensors used in this validation (T1 and T11 in Figure 1) are installed at a certain distance from the compressors, with pipe insulation of industrial quality (with the main purpose of avoiding injuries due to accidental contact)

and are on the pipe surface. We also evaluated whether the compressor models should be corrected to account for this heat loss or temperature drop, which could affect the amount of heating available in the integrated system for DHW production or RTUs. However, 5 K at the area where the compressor discharge is, e.g., at 80 bar or 100 bar, corresponds to a less than 10 kJ/kg enthalpy drop, which can be neglected considering that an enthalpy difference of even more than 200 kJ/kg is available for heating in transcritical operation.
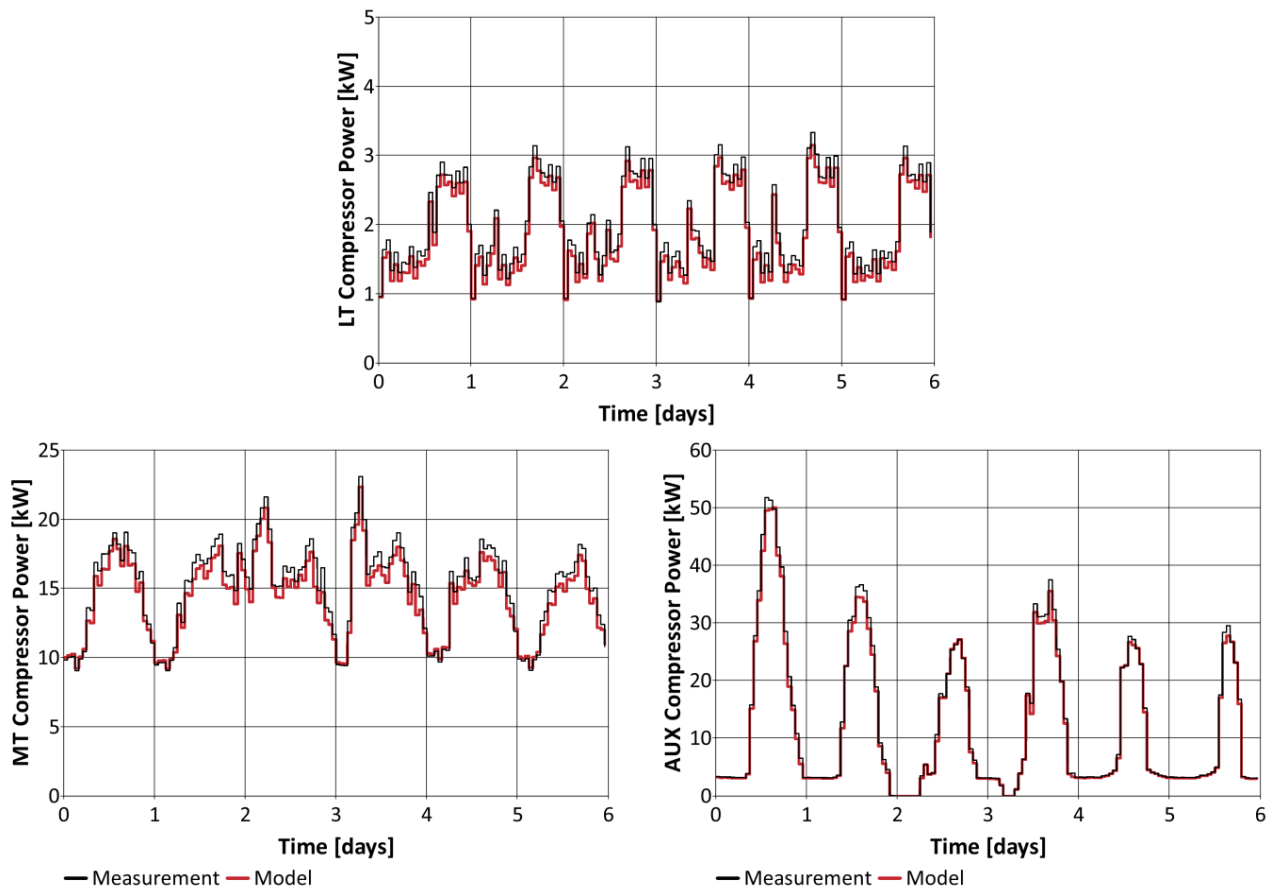

Figure 7. Validation results for the compressor modeling approach; comparison between measured (black) vs. calculated (red) compressor power values in kW for LT, MT, and AUX compressors.
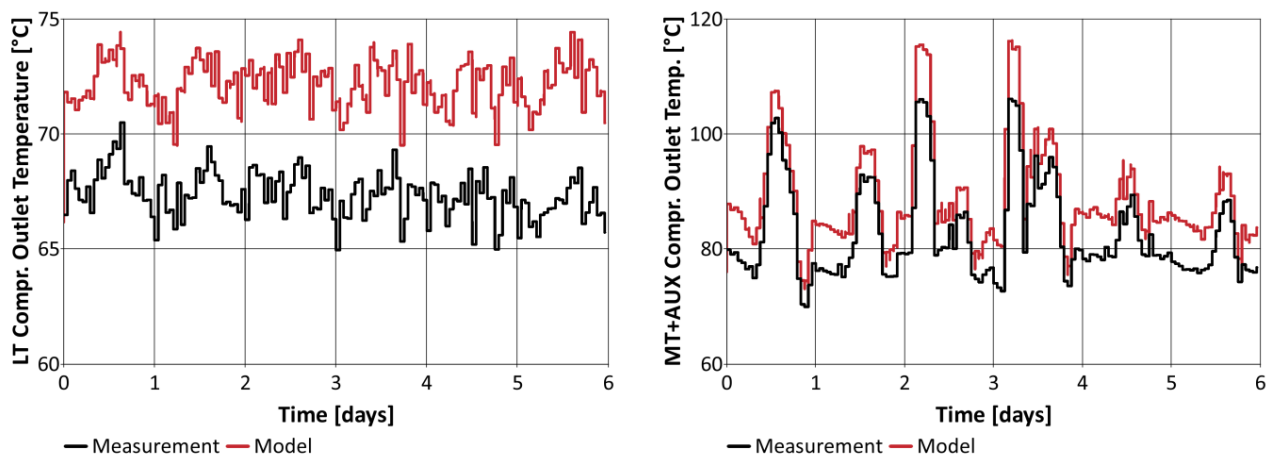

Figure 8. Validation results for the compressor modeling approach; comparison between calculated vs. measured compressor outlet temperature in °C for LT and MT + AUX compressors.

4.2. System Validation

The quality of the overall system model presented in Figure 2 was assessed in this section. First, the power consumption of the different compressor groups (LT, MT, and AUX) obtained with the Modelica model was compared with the experimental data registered during the week used for validation (2019, week 34), as described in Section 2.2. it must be noted that the integrated CO_2 refrigeration system was operated with a high-pressure (HP) ejector block and a disabled low-pressure lift (AC) ejector and liquid ejector, i.e., operating with direct-expansion RTU and MT evaporators.

The results of this validation are shown in Figure 9. The main conclusions drawn from the validation are listed below:

- Measurement data are averaged every hour, while those from the simulation show the output every 10th min. Thus, the model depicts the cycling of compressors that is a consequence of a non-optimal selection and sizing of the compressor installed in each group, with relevant capacity gaps (Table 1 and Figure 4).
- There is good agreement between experimental and numerical power consumption for the LT compressors. During this week, the average experimental result is 2.01 kW, while the numerical result is 1.86 kW (an approximate 7.5% discrepancy).
- The model underestimates the MT compressor power consumption measured by 19.4% on average (from 12.17 kW to 15.10 kW), which is not negligible. On the other hand, it overestimates the power consumption of the auxiliary compressors by 9% on average (13.58 kW vs. 12.46 kW). There are two main explanations for this disagreement. First, that the ejector could be performing slightly worse than indicated by the models (either the detailed model or the polynomial based model). It is worth noting that the ejector models are based on experimental data at the ejector cartridge level, and integration within the block (Multi Ejector) could slightly reduce the efficiency [34,35]. Second, the FGBV was utilized more often in the actual system than predicted by the model. This would be a consequence of the previous explanation and of a more conservative strategy of the system controller, which would only enable AUX compressors with a sufficient margin of flash gas in the receiver, while the model control strategy would be more aggressive. In both cases, the distribution of load between MT and AUX compressors is affected, reducing the requested MT compressor capacity in favor of AUX compressors.
- The total compressor power consumption is also represented for the whole validation period, from the experimental data and from the model. The average experimental and numerical values are 29.58 kW and 27.61 kW, respectively, with the deviation being around 6.7%. This is within the given uncertainties for refrigerant mass flow, electric power consumption measurements, and the uncertainty related to the applied compressor polynomials as defined in EN 12900:2013 [25].

From the previous points, it could be concluded that the dynamic model represents the real behavior of the case study with acceptable accuracy.

Figure 10 represents the system COP during the whole validation period determined by the experimental data and the numerical results. The system COP is evaluated at a certain time as the sum of the thermal loads (MT, LT, AC, and DHW), divided by the total compressor power consumption (MT, LT, and AUX). The average discrepancy between numerical and experimental COP accounts for approximately 10% (3.42 vs. 3.10) in the validation.
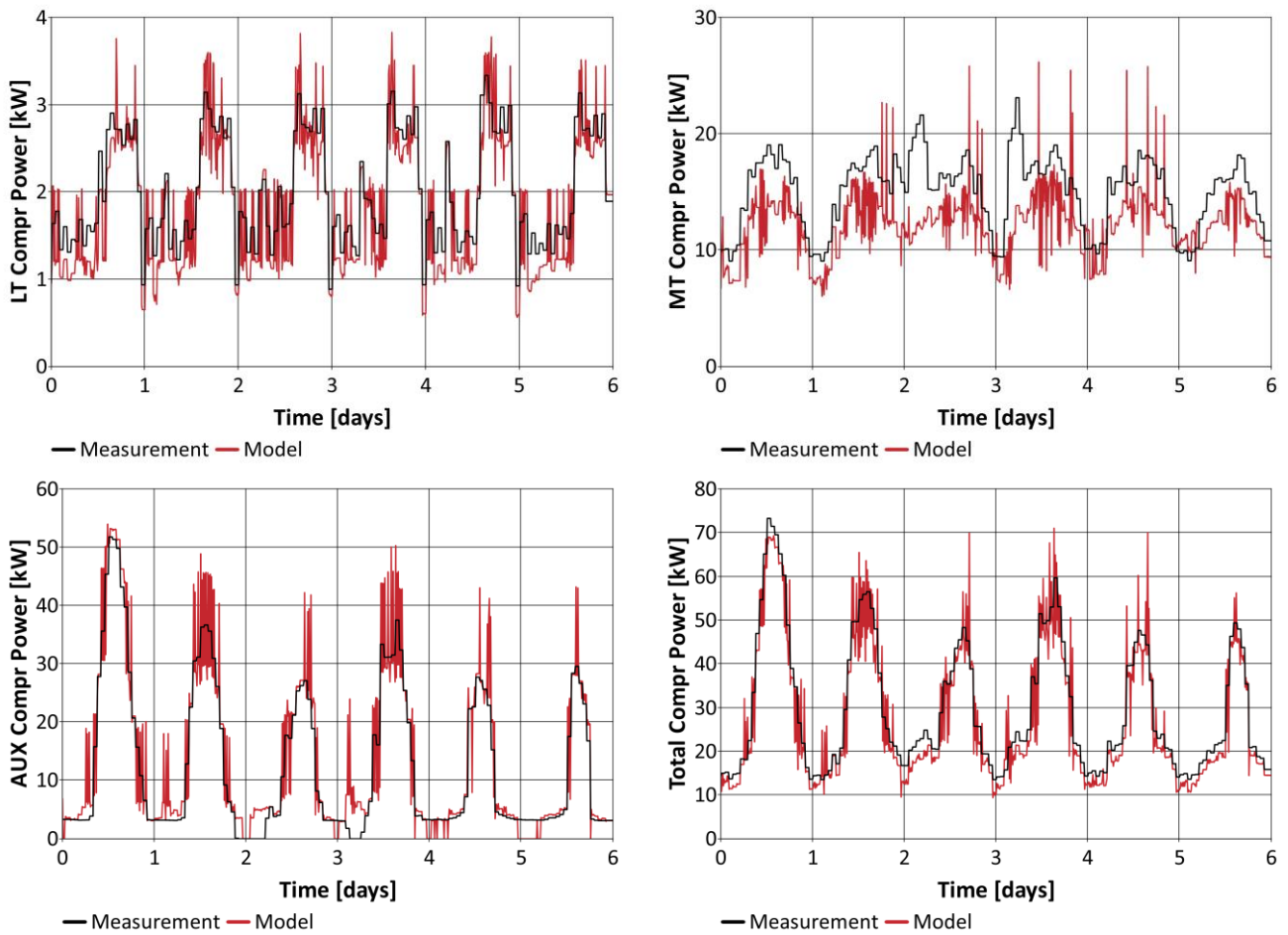
Figure 9. Validation results for the system model based on measurements for the system operating with HP ejector block during a summer week in 2019 (week 34); comparison between measured (black) vs. calculated (red) power consumption for LT, MT, and AUX compressors, as well as the total for all compressor groups.
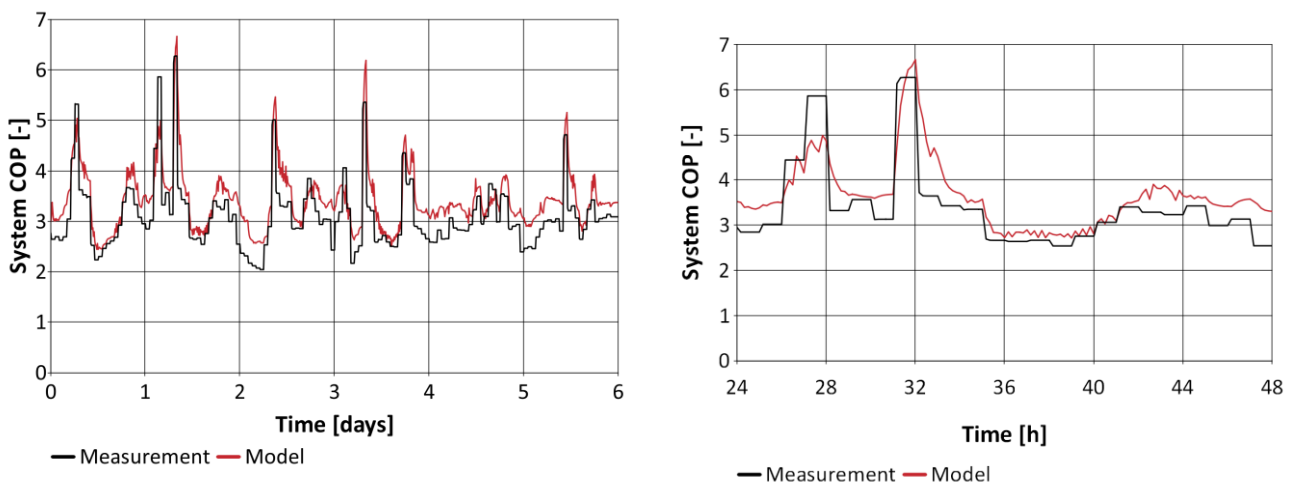

Figure 10. System COP, experimental (black) and numerical (red) for the whole validation period (**left**), and for the second day of that period (**right**).

4.3. System Performance Assessment

4.3.1. HP Ejector-Supported System vs. HPV System

The validated Modelica model was used to directly quantify the benefits of the HP ejector used in the integrated system on the system COP. In the following subsections, system COP was evaluated accounting for cooling loads and heating loads, which in this case was DHW production. The model offers the possibility to assess different operation modes under the same boundary conditions, which would be challenging to achieve on a real supermarket site such as Porto de Mos due to constantly fluctuating boundary conditions between several days regarding the ambient temperature or internal heating/cooling demands. For this purpose, the system model was adapted so that the "ejector-less" system had the HP ejector disabled/removed, while high-pressure control was the responsibility of the HPV only.

Figure 11 shows the resulting system COP curves and percentage increase in COP due to HP ejector use, for the same week that was presented for the validation (week 34 in 2019). The HP ejector's ability to transfer load from the MT to AUX compressors means that the FGBV is almost unnecessary in the removal of the flash gas from the receiver and the regulation of its pressure. In the configuration with HPV only, the FGBV is much more present, which has a negative effect on system COP and on the use of the AUX compressors. On average, during the period investigated, the system COP is improved by 5.81% with the HP ejector compared to the ejector-less system with identical boundary conditions (ambient temperatures and loads). The most important benefits occur, as would be expected, when the ambient temperature is higher, in the middle of the day. However, it is worth noting that the summer week taken for validation is mild considering the location of the system, as represented by the gas cooler outlet temperature represented in red in Figure 11 (right). Higher benefits would be expected on warmer days and if the ejector technology was combined with a smart receiver pressure control or a flooded MT evaporator, as investigated in the following subsections.
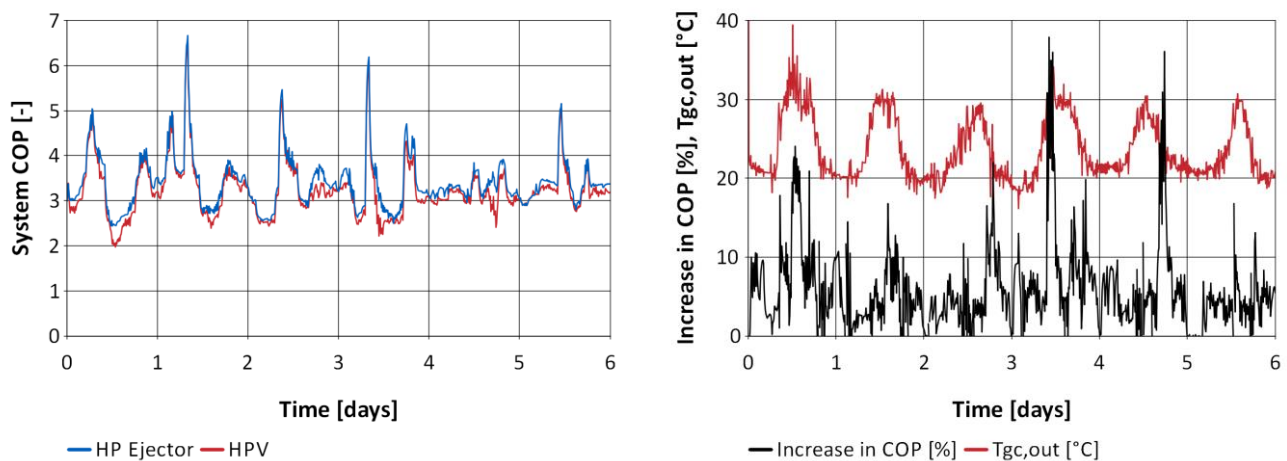

Figure 11. System COP in the case the HP ejector is utilized compared with the ejector-less configuration (**left**) and increase in system COP as a function of gas cooler outlet temperature (**right**).

4.3.2. Receiver Pressure Setpoint on HP Ejector-Supported Integrated System

The receiver pressure setpoint may be relevant to the performance of conventional transcritical CO_2 refrigeration systems, but it becomes crucial in integrated CO_2 refrigeration systems. The reason is that the receiver pressure is closely associated with AC production, either because the AC evaporators/RTUs operate at that pressure level, which is the case analyzed in detail in this paper, or because they are linked to it through an ejector and its pressure lift, which is the alternative that was presented in Section 2.1.

The validated model was utilized to analyze the influence of the receiver pressure setpoint on the system COP during the dynamic simulations. Three scenarios were considered: (i) A fixed setpoint at 35 bar (a saturation temperature of around 0 °C and an HP ejector pressure lift around 8 bar); (ii) a fixed setpoint at increased pressure such as 40 bar (a saturation temperature of around 5 °C and an HP ejector pressure lift around 13 bar); and (iii) a floating setpoint dependent on the gas cooler outlet temperature between the previous setpoints, 35 bar and 40 bar. The first scenario is the setpoint programmed in the system during the validation week (week 34 in 2019) and is used as a reference. The second should lead to a sufficiently low evaporation temperature for AC production (5 °C evaporation temperature). The third is conceived for more efficient use of the HP ejector, better adapting the most efficient pressure lift (highest ejector efficiency) to the gas cooler outlet conditions. In all cases, the MT evaporators operate as dry expansion at 27.2 bar (−9 °C evaporation temperature).

The results of this analysis are included in Figure 12. Increasing the receiver setpoint from 35 bar to 40 bar has a different impact depending on the conditions. A higher receiver pressure (40 bar) is particularly convenient when there is AC demand and a warmer temperature outdoors, which leads to a higher HP ejector motive nozzle temperature. The system COP can increase over 10% compared to the reference case of the 35 bar receiver pressure setpoint during those periods, but it can also be penalized by the same amount at others, due to less favorable operating conditions for the HP ejector and a reduced amount of flash gas to keep AUX compressors running.
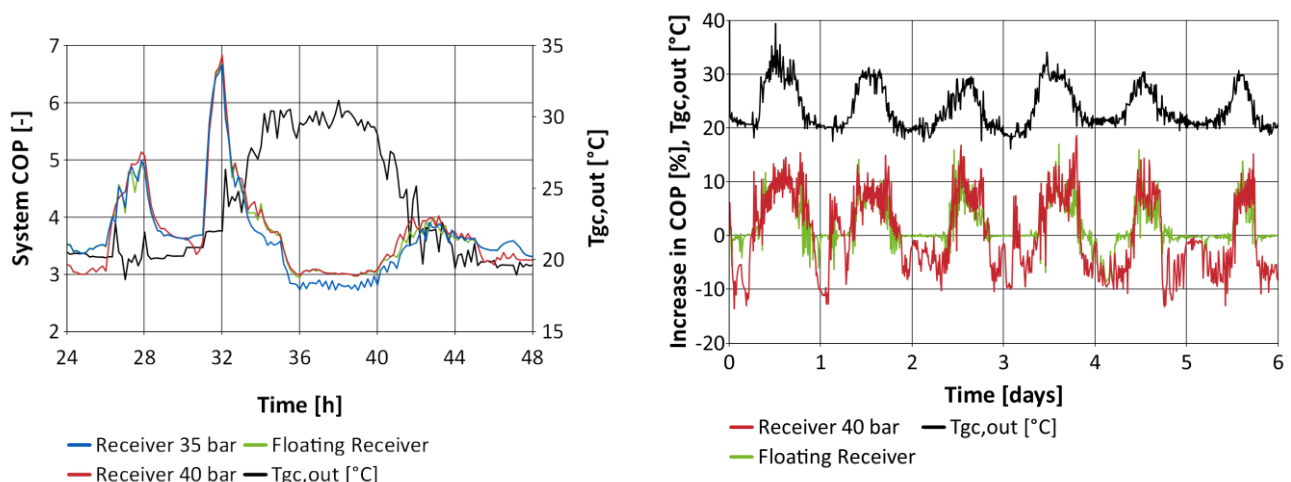

Figure 12. Analysis of strategies for receiver pressure control in integrated CO_2 refrigeration systems with HP ejector. (**Left**) Evolution of the system COP during a day with the different setpoints. (**Right**) Increase in COP during the reference week on the basis of the HP ejector system with 35 bar setting.

The floating receiver setpoint approach appears to be more convenient for the changing environmental conditions that exist with integrated CO_2 refrigeration systems, as shown in Figure 12. It combines the COP enhancement at warmer conditions with no deterioration at colder temperatures and lower AC demands. From the HP ejector with a fixed setpoint at 35 bar to a controlling strategy with a floating receiver pressure, the average system COP increase in the reference week goes from 5.81% to 8.01%, using the HPV layout (ejector-less) as a reference.

4.3.3. Flooded Evaporators with Liquid Ejector

Flooded evaporation to increase evaporation temperature is seen as critical for improving the competitiveness of integrated CO_2 refrigeration systems under any climatic conditions. The demonstration site presented in this case study has been dimensioned for flooded MT evaporation at −4 °C with liquid ejectors as compressor protection. However, in the week used for model validation, it was operated with direct expansion and an MT

evaporation temperature of $-9\,°C$. Assuming a liquid ejector efficiency of 10% in the validated model (see Section 3.3), it was possible to numerically evaluate the effect of this MT evaporation temperature increase at 5 K. In addition, two strategies were analyzed following the study on the receiver pressure setpoint indicated in the previous subsection: (i) A fixed setpoint at 40 bar, which leads to a relatively constant HP ejector pressure lift close to 9 bar; and (ii) a floating setpoint between 38 bar and 43 bar, with an ejector pressure lift between 7 bar and 12 bar. This last scenario assumes that an evaporation pressure of 43 bar (a saturation temperature around $8\,°C$) is sufficiently low for the RTUs to provide air conditioning, which in the end is a matter of heat exchanger sizing.

As depicted in Figure 13, the system COP is consistently higher with flooded evaporation and ejectors than with the HPV configuration (ejector-less), independently of the strategy adopted for receiver pressure control. Considering a constant receiver setpoint, the average COP enhancement compared with the HPV system layout is 13.13%. An additional improvement is achieved with floating setpoint control at the warmest periods of the day, reaching 15.16% compared with the HPV system. The reason for this is the combination of a better ejector efficiency at those conditions and a higher evaporation temperature for the RTUs.
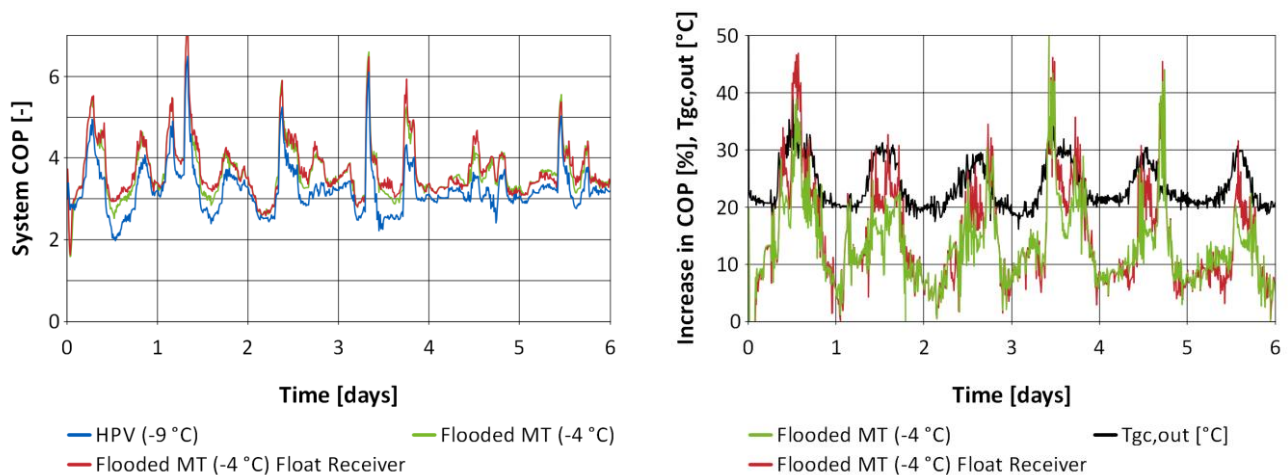

Figure 13. Analysis of the effect of MT flooded evaporation on system performance, both with fixed and floating receiver setpoints. (**Left**), system COP for HPV system compared to ejector-supported flooded evaporation. (**Right**), increase in COP during the reference week on the basis of the HPV system layout.

4.3.4. Synopsis of the Comparison between Configurations

This subsection uses Table 4 to summarize the previous findings and comparisons between system configurations in the average period investigated in this case study. It should give an idea of the potential of the different technologies to improve the COP of the system based on the validated numerical model.

Table 4. Summary table of the average system COPs for the different configurations of CO_2 integrated refrigeration system and increase in COP (%) compared with the ejector-less (HPV) system layout.

Configuration	System COP	Increase COP (%)
HPV	3.24	-
HP Ej., Receiver 35 bar	3.42	6
HP Ej., Floating Receiver	3.48	8
HP & Liq. Ej., Receiver 40 bar	3.66	13
HP & Liq. Ej., Floating Receiver	3.72	15

4.3.5. Discussion of Results with Other Studies in the Literature

The COP improvements, up to 8%, determined experimentally by Haida et al. (2016) [36] with the utilization of vapor ejectors (compared to the system with parallel compression, HPV, and MT load only) are in the same order of magnitude as those evaluated in the present study. Their experimental data also showed the importance of receiver pressure on the system performance, affecting the efficiency of compressors and ejectors. The numerical investigation by Gullo et al. [37] analyzed different system configurations, including a parallel compression booster system with and without a Multi Ejector. As in one of the cases of the present study, the work by Gullo considered flooded MT evaporation at $-4\,^\circ$C in the case with the ejector. For the city of Lisbon, Gullo and co-authors determined a 17% annual energy consumption reduction due to the implementation of an ejector and flooded MT evaporation to the parallel compression booster system. This value seems high compared to the results obtained in the present study, which correspond to a week in summer when the performance of the ejector should be highest. However, it is important to highlight that the values of ejector efficiency in [37] (defined through the entrainment ratio) were particularly high at relatively low ambient conditions (external air temperature less or equal than 17 $^\circ$C), which does not relate to our field experience. Pisano [38] evaluated annual energy savings in an Italian supermarket of around 20% due to the implementation of vapor and liquid ejectors (and flooded MT evaporation) compared to the parallel compression booster system. In the same line, higher energy savings than in the current study were observed by Madsen and Kriezi (2018) [8], with annual energy savings between 17% and 29% (compared to a booster system), depending on the average annual temperature at the location. On the other hand, in Kriezi et al. (2018) [13], it was concluded that lower COP improvements by ejector implementation were determined from field measurements (June to August 2017) than from numerical studies, which is also the case for the current study using a model validated with field data. The field tests from an ejector-supported booster system in Switzerland, reported in Hafner et al. [39], not only showed the positive effect of an increased evaporation temperature on system efficiency but also the drastic reduction of frost formation and defrost cycles. Reduced defrosting needs were also encountered in the Porto de Mos supermarket in the present case study. The field results from Fredslund et al. [40] indicated relatively low energy reductions due to ejector implementation, approximately 4% and 14% without and with AC integration, respectively, in the same line as the current study.

5. Conclusions

Integrated CO_2 refrigeration systems have the potential to reduce energy consumption and save costs for shop owners if intended to meet the complete HVAC&R demands of the supermarket. A numerical model of such a CO_2 system was developed in Modelica programming language to replicate one of the demonstration sites within the EU project MultiPACK: A CO_2 refrigeration system located in Porto de Mos (Portugal), equipped with the latest technological advancements for performance enhancement (parallel compression, ejectors, flooded evaporators, etc.) and well instrumented with power meters, mass flow meters, pressure transducers, and temperature sensors at strategic locations. The model was validated with acceptable accuracy for the considered summer period. The aim of the model was to be able to evaluate and compare the performance of the system when utilizing the various system configurations presented in the paper, while still maintaining comparable boundary conditions between the cases. The conclusions that can be drawn from this analysis are listed below:

- The validation of the dynamic model has shown an average discrepancy of 10% in terms of system COP, which can be explained by (i) the slight overprediction of the ejector performance; (ii) the different receiver pressure control parameters, which require the model to anticipate the use of the AUX compressors earlier than it happens in the real installation; and (iii) the uncertainties inherent to the compressor polynomials used in the model. However, this value is considered acceptable for the purpose of this model.

- The HP ejector efficiency is typically above 20% with the relatively warm external conditions existing in this case study, which are not uncommon for the location. The repercussion of HP ejector implementation in the system COP is approximately 6% compared with the ejector-less scenario (HPV-only) during the studied week. Larger improvements would be expected during a significant part of the year with higher ambient temperatures.
- The increase in the MT evaporation temperature with flooded evaporation is possible without risk to the compressors due to the use of liquid ejectors. The combined effect of the HP ejector and the 5 K evaporation temperature increase (with a liquid ejector) on system COP is 13% compared to the HPV-only system layout during the week used for validation. Since there is also a liquid ejector design for low motive nozzle conditions, i.e., cold or mild outdoor temperatures, the enhancement of COP due to the evaporation temperature increase should be expected all year long.
- A convenient regulation of the receiver pressure, with a floating setpoint function of the environmental conditions, is important to operate the ejectors with higher efficiency. This has a positive effect on the system COP throughout the day.

In the future, the newly derived and validated Modelica system model can be further used to investigate additional system components (e.g., a low-pressure ejector), different component dimensions, or new control strategies.

References

1. UNIDO. The Montreal Protocol Evolves to Fight Climate Change. Available online: https://www.unido.org/our-focus-safeguarding-environment-implementation-multilateral-environmental-agreements-montreal-protocol/montreal-protocol-evolves-fight-climate-change (accessed on 31 August 2021).
2. Ciconkov, R. Refrigerants: There is still no vision for sustainable solutions. *Int. J. Refrig.* **2018**, *86*, 441–448. [CrossRef]
3. Gullo, P.; Tsamos, K.M.; Hafner, A.; Banasiak, K.; Ge, Y.T.; Tassou, S.A. Crossing CO_2 equator with the aid of multi-ejector concept: A comprehensive energy and environmental comparative study. *Energy* **2018**, *164*, 236–263. [CrossRef]
4. Hafner, A.; Pardiñas, Á.Á. CO_2 Refrigeration Technology: Possible Innovations. In Proceedings of the 8th Conference on Ammonia and CO_2 Refrigeration Technology, Ohrid, Macedonia, 11–13 April 2019. [CrossRef]
5. Koegelenberg, I. *World Guide to Transcritical CO_2 Refrigeration*; Shecco: Brussels, Belgium, 2020.
6. Minetto, S.; Marinetti, S.; Saglia, P.; Masson, N.; Rossetti, A. Non-technological barriers to the diffusion of energy-efficient HVAC&R solutions in the food retail sector. *Int. J. Refrig.* **2018**, *86*, 422–434. [CrossRef]
7. Coulomb, D.; Colombo, I.; Claussen, I.C.; Kauko, H.; Kerstin, M.; Belluomini, D. Achievements of the SuperSmart EU project. *Int. J. Refrig.* **2019**, *98*, v–vii. [CrossRef]
8. Madsen, K.B.; Kriezi, E.E. Financial Aspects of Ejector Solutions in Supermarket and Smaller Industrial Systems. In Proceedings of the 13th IIR Gustav Lorentzen Conference on Natural Refrigerants (GL2018), Valencia, Spain, 18–20 June 2018. [CrossRef]
9. Kriezi, E.E.; Fredslund, K.; Banasiak, K.; Hafner, A. R744 Multi Ejector Development. In Proceedings of the 12th IIR Gustav Lorentzen Natural Working Fluids Conference, Edinburgh, Scotland, 21–24 August 2016. [CrossRef]
10. Gullo, P.; Hafner, A.; Banasiak, K.; Minetto, S.; Kriezi, E.E. Multi-Ejector Concept: A Comprehensive Review on its Latest Technological Developments. *Energies* **2019**, *12*, 406. [CrossRef]
11. Karampour, M.; Sawalha, S. State-of-the-art integrated CO_2 refrigeration system for supermarkets: A comparative analysis. *Int. J. Refrig.* **2018**, *86*, 239–257. [CrossRef]

12. Hafner, A.; Nekså, P. Integrated CO$_2$ Solutions for Supermarkets. In Proceedings of the 13th IIR Gustav Lorentzen Conference on Natural Refrigerants (GL2018), Valencia, Spain, 18–20 June 2018. [CrossRef]

13. Kriezi, E.E.; Larsen, L.F.S.; Piscopiello, S.; Madsen, K.B. System Efficiency and Energy Savings with Parallel Compression and Ejectors under Flooded Conditions. In Proceedings of the 13th IIR Gustav Lorentzen Conference on Natural Refrigerants (GL2018), Valencia, Spain, 18–20 June 2018. [CrossRef]

14. Hafner, A. Integrated CO$_2$ System Refrigeration, Air Conditioning and Sanitary Hot Water. In Proceedings of the 7th Conference on Ammonia and CO$_2$ Refrigeration Technology, Ohrid, Macedonia, 11–13 May 2017. [CrossRef]

15. Nekså, P.; Girotto, S.; Schiefloe, P.A. Commercial Refrigeration using CO$_2$ as Refrigerant: System Design and Experimental Results. In Proceedings of the Natural Refrigerants, Energy Efficiency, Cost and Safety. Natural Working Fluids '98, IIR-Gustav Lorentzen Conference, Oslo, Norway, 2–5 June 1998.

16. MultiPACK. «MultiPack—Horizon 2020 Research and Innovation Programme» Project Number 723137. Available online: https://www.ntnu.edu/multipack (accessed on 31 August 2021).

17. D'Agaro, P.; Coppola, M.A.; Cortella, G. Field tests, model validation and performance of a CO$_2$ commercial refrigeration plant integrated with HVAC system. *Int. J. Refrig.* **2019**, *100*, 380–391. [CrossRef]

18. Minetto, S.; Tosato, G.; Rossetti, A.; Marinetti, S.; Girotto, S.; Banasiak, K. Not-in-kind Approach to Remote Monitoring in CO$_2$ Refrigeration Systems. In Proceedings of the 25th IIR International Congress of Refrigeration, Montréal, QC, Canada, 24–30 August 2019. [CrossRef]

19. Gullo, P.; Hafner, A.; Banasiak, K. Transcritical R744 refrigeration systems for supermarket applications: Current status and future perspectives. *Int. J. Refrig.* **2018**, *93*, 269–310. [CrossRef]

20. Dassault Systems—DYMOLA. Systems Engineering. Available online: https://www.3ds.com/products-services/catia/products/dymola (accessed on 6 June 2017).

21. Association Modelica. Modelica. Available online: https://modelica.org/ (accessed on 31 August 2021).

22. Gräber, M.; Kosowski, K.; Richter, C.; Tegethoff, W. Modelling of heat pumps with an object-oriented model library for thermodynamic systems. *Math. Comput. Model. Dyn. Syst.* **2010**, *16*, 195–209. [CrossRef]

23. TLK-Thermo GmbH. TIL Suite Thermal Systems. Available online: https://www.tlk-thermo.com/index.php/en/til-suite (accessed on 31 August 2021).

24. Bitzer. Software v6.5.0 rev1610. Available online: https://www.bitzer.de/websoftware/ (accessed on 31 August 2021).

25. European Committee for Standardization. *EN 12900:2013 Refrigerant Compressors—Rating Conditions, Tolerances and Presentation of Manufacturer's Performance Data*; Standard Norge: Oslo, Norway, 2013.

26. Lawrence, N.; Elbel, S. Theoretical and practical comparison of two-phase ejector refrigeration cycles including First and Second Law analysis. *Int. J. Refrig.* **2013**, *36*, 1220–1232. [CrossRef]

27. Elbel, S.; Hrnjak, P. Experimental validation of a prototype ejector designed to reduce throttling losses encountered in transcritical R744 system operation. *Int. J. Refrig.* **2007**, *31*, 411–422. [CrossRef]

28. Hafner, A.; Banasiak, K. Full Scale Supermarket Laboratory R744 Ejector Supported & AC Integrated Parallel Compression Unit. In Proceedings of the 12th IIR Gustav Lorentzen Conference on Natural Refrigerants (GL2016), Edinburgh, Scotland, 21–24 August 2016. [CrossRef]

29. Haida, M.; Smolka, J.; Hafner, A.; Ostrowski, Z.; Palacz, M.; Nowak, A.J.; Banasiak, K. System model derivation of the CO$_2$ two-phase ejector based on the CFD-based reduced-order model. *Energy* **2018**, *144*, 941–956. [CrossRef]

30. Haida, M.; Fingas, R.; Szwajnoch, W.; Smolka, J.; Palacz, M.; Bodys, J.; Nowak, A.J. An Object-Oriented R744 Two-Phase Ejector Reduced-Order Model for Dynamic Simulations. *Energies* **2019**, *12*, 1282. [CrossRef]

31. Haida, M.; Smolka, J.; Hafner, A.; Palacz, M.; Ostrowski, Z.; Bodys, J.; Kriezi, E.K.; Försterling, S.; Nowak, A.J.; Banasiak, K. Performance operation of liquid ejectors for a R744 integrated multi-ejector supermarket system using a hybrid ROM. *Int. J. Refrig.* **2020**, *110*, 58–74. [CrossRef]

32. Haida, M.; Smolka, J.; Hafner, A.; Ostrowski, Z.; Palacz, M.; Madsen, K.B.; Försterling, S.; Nowak, A.J.; Banasiak, K. Performance mapping of the R744 ejectors for refrigeration and air conditioning supermarket application: A hybrid reduced-order model. *Energy* **2018**, *153*, 933–948. [CrossRef]

33. Brennen, C. *Fundamentals of Multiphase Flow*; Cambridge University Press: Cambridge, UK, 2005.

34. Banasiak, K.; Hafner, A.; Kriezi, E.E.; Madsen, K.B.; Birkelund, M.; Fredslund, K.; Olsson, R. Development and performance mapping of a multi-ejector expansion work recovery pack for R744 vapour compression units. *Int. J. Refrig.* **2015**, *57*, 265–276. [CrossRef]

35. Khorshidi, V.; Kriezi, E.E.; Schlemminger, C.; Hafner, A. Performance of Integrated R744 Packs Part 2—Ejectors Performance, a Comparison of Data-Driven Model from Onsite Measurements with ROM Model Predictions. In Proceedings of the 10th IIR Conference on Compressors and Refrigerants, Bratislava, Slovakia, 13 January 2021. [CrossRef]

36. Haida, M.; Banasiak, K.; Smolka, J.; Hafner, A.; Eikevik, T.M. Experimental analysis of the R744 vapour compression rack equipped with the multi-ejector expansion work recovery module. *Int. J. Refrig.* **2016**, *64*, 93–107. [CrossRef]

37. Gullo, P.; Hafner, A.; Cortella, G. Multi-ejector R744 booster refrigerating plant and air conditioning system integration—A theoretical evaluation of energy benefits for supermarket applications. *Int. J. Refrig.* **2017**, *75*, 164–176. [CrossRef]

38. Pisano, G. The Use of Ejectors Technology: How to Boost Efficiency in Warm Climates—A Real Example from Italy. In Proceedings of the 13th IIR Gustav Lorentzen Conference on Natural Refrigerants (GL2018), Valencia, Spain, 18–20 June 2018. [CrossRef]
39. Hafner, A.; Schönenberger, J.; Banasiak, K.; Girotto, S. R744 Ejector Supported Parallel Vapour Compression Systems. In Proceedings of the 3rd IIR International Conference on Sustainability and the Cold Chain, London, UK, 23–25 June 2014.
40. Fredslund, K.; Kriezi, E.E.; Madsen, K.B.; Birkelund, M.; Olsson, R. CO_2 Installations with a Multi Ejector for Supermarkets, Case Studies from Various Locations. In Proceedings of the 12th IIR Gustav Lorentzen Natural Working Fluids Conference, Edinburgh, Scotland, 21–24 August 2016. [CrossRef]